6

Decoupling of Multivariable Systems and Application to Flight Control System

Tain-Sou Tsay

Department of Aeronautical Engineering, National Formosa University

Abstract

In this literature, an effective decoupling method is proposed for analyses and designs of multivariable systems. It is applied to a serious aerodynamic coupled missile flight control system. No matrix inversion of the system dynamic for decoupling control is required. From frequency and time responses of the illustrating multivariable example, it will be seen that the decoupling and robustness for aerodynamic couplings can be obtained simultaneously. The decoupling effects are kept almost unchanged for large system parameter variations and uncertainties.

Keywords: Multivariable Systems Decoupling、Flight Control System.

I. Introduction

The flight control systems are widely used real multivariable feedback control systems. They are large parameter variation systems for large flight envelope and serous cross-coupling systems for aerodynamic couplings. For skid-to-turn(STT) missile flight control systems, aerodynamic couplings from pitching/ yawing channels to rolling channel are destabilizing and degrade performance of the system [1,2]. Higher gain crossover frequency ratios of the rolling channel to pitching/ yawing channels are usually expected. They are usually used in conventional design techniques [3,4], and are diagonal dominant designs for multivariable feedback systems [5,6]. However, it is constrained by hardware dynamics and system requirements for target engaging. Other possible methods are to use cross-decoupling controllers [7-9] and output feedback- decoupling controllers [10,11]. In general, inverting the transfer function matrix of multivariable plant suffers from it may have large modeled, un-modeled uncertainties, non-minimum phase zeros and large faster variations of cross-coupling dynamics.

Dynamic Inversion(DI) is another possible methodology for designing multivariable control laws [12-18]. A DI controller consists of two parts. In inner loop, nonlinear input-output behavior of the plant is canceled by feedback control laws, consisting of inverse nonlinear model equations. The closed-loop system is reduced to a set of integrators. In outer loop, a linear controller is used to impose desired command response behavior. Unfortunately, dynamic inversion control laws may show very poor robustness to uncertainties in the designing model. This problem is usually coped with by introducing robustness design techniques: H_∞ / μ synthesis [16], Quantitative Feedback Theory (QFT) [16, 17], Structured Singular Value Synthesis (SSV) [18], etc. to find robust controllers for recovering the required robustness under model uncertainties.

In this literature, a nonlinear decoupling method is proposed for multivariable feedback control systems. Decoupling is derived from multiplications of measurable output feedback datum and controllable outputs of conventional diagonal controllers. No matrix inversion for plant dynamic is need in analysis and designs. The decoupling behaviors are nonlinear, and will be linearized by small perturbation theorem. It is similar to find the linearized model of the plant. Exact decoupling and diagonal dominant conditions are formulated.

The proposed method is applied to a supersonic-missile flight control system. It is a 3×3 multivariable feedback control system with lager parameter variations. Multiplications of two measurable accelerations with three controllable outputs of conventional well-proven autopilot are used to cope with aerodynamic couplings. They offer exact sign and magnitude proportional to aerodynamic coupling. Over or wrong cancellation can be prevented. It needs not to concern the internal stability [7-9]. The magnitudes of decoupling terms will be found by eliminating major coupling elements of the state transition matrix of a simplified coupled system only. The validation of simplification is verified by the completed system including hardware dynamics and compensations. From frequency responses of uncoupled, coupled and decoupled systems, it will be seen that the decoupling and robustness coped with aerodynamic couplings can be obtained simultaneously. All analyzed results will be verified by 5-DOF digital simulations under large parameter variations and uncertainties.

II. The Proposed Decoupling Method

Considering a general $m \times m$ multivariable system described below:

$$\dot{X} = f(X, U_{(m \times 1)}, t) \tag{1}$$
$$Y_{(m \times 1)} = g(X, U_{(m \times 1)}, t)$$

If diagonal controllers $p_1(s), p_2(s),.., p_m(s)$ were used, then inputs of multivariable system are

$$U_{(m \times 1)} = diag[p_1(s), p_2(s),.., p_m(s)]\big(R_{(m \times 1)} - Y_{(m \times 1)}\big) \tag{2}$$

where $R_{(m \times 1)}$ are input commands. Eq. (2) represents conventional designs without cross-coupling controllers. For illustrating the proposed decoupling method, 3×3 multivariable systems will be discussed and applied to a 3×3 flight control system. The three inputs (U_1, U_2, U_3) given in Eq. (2) are replaced by (U_1', U_2', U_3') and given below:

$$U_1' = U_1 + K_{23}U_2Y_3 + K_{32}U_3Y_2$$
$$U_2' = U_2 + K_{13}U_1Y_3 + K_{31}U_3Y_1 \tag{3}$$
$$U_3' = U_3 + K_{12}U_1Y_2 + K_{21}U_2Y_1$$

The added terms to original (U_1, U_2, U_3) are decoupling terms. For instance, $K_{23}U_2Y_3$ and

6

$K_{32}U_3Y_2$ are decoupling control for coping with coupling from channels 2 and 3 to channel 1. The command U'_1 includes feed-forward (U_2, U_3) and feedback (Y_2, Y_3) decoupling behaviors. $K_{ij,i \neq j}$ are parameters to be found. Eq. (3) gives that (Y_1, Y_2, Y_3) are three measurable output feedback datum and (U'_1, U'_2, U'_3) are three controllable datum. Certainly, one can use U_1Y_1, U_2Y_2, and U_3Y_3 in Eq. (3) for decoupling. But, it will be seen that Eq. (3) is the good decoupling formulation for flight control systems.

The nth-order small signal perturbation model from a specified set of trim conditions $\overline{U}'_{(3 \times 1)}$ and $\overline{Y}_{(3 \times 1)}$ of Eq. (1) for 3×3 multivariable systems are

$$\dot{X}_{(n \times 1)} = A_{(n \times n)}X_{(n \times 1)} + B_{(n \times 3)}u'_{(3 \times 1)} \qquad (4)$$
$$y_{(3 \times 1)} = C_{(3 \times n)}X_{(n \times 1)} + D_{(m \times 3)}u'_{(3 \times 1)}$$

for $(U'_i = \overline{U}'_i + u'_i; i = 1,2,3)$ and $(Y_i = \overline{Y}_i + y_i; i = 1,2,3)$. The small perturbed models of Eq. (3) derived from trim conditions ($\overline{U}_1, \overline{U}_2, \overline{U}_3$), ($\overline{U}'_1, \overline{U}'_2, \overline{U}'_3$) and ($\overline{Y}_1, \overline{Y}_2, \overline{Y}_3$) are

$$u'_1 = u_1 + K_{23}(\overline{U}_2 y_3 + \overline{Y}_3 u_2) + K_{32}(\overline{U}_3 y_2 + \overline{Y}_2 u_3)$$
$$u'_2 = u_2 + K_{13}(\overline{U}_1 y_3 + \overline{Y}_3 u_1) + K_{31}(\overline{U}_3 y_1 + \overline{Y}_1 u_3)$$
$$u'_3 = u_3 + K_{12}(\overline{U}_1 y_2 + \overline{Y}_2 u_1) + K_{21}(\overline{U}_2 y_1 + \overline{Y}_1 u_2)$$
$$(5)$$

for $(U_i = \overline{U}_i + u_i; i = 1,2,3)$. For simplicity, constant diagonal gains $diag\{p_1, p_2, p_3\}$ are used. Input commands $[R_1, R_2, R_3]^T$ are set to be zeros for general use. Then, Eq. (5) can be rewritten as

$$\begin{bmatrix} u'_1 \\ u'_2 \\ u'_3 \end{bmatrix} = \begin{bmatrix} -p_1 & -K_{23}\overline{Y}_3 p_2 + K_{32}\overline{U}_3 & -K_{32}\overline{Y}_2 p_3 + K_{23}\overline{U}_2 \\ -K_{13}\overline{Y}_3 p_1 + K_{31}\overline{U}_3 & -p_2 & -K_{31}\overline{Y}_1 p_3 + K_{13}\overline{U}_1 \\ -K_{12}\overline{Y}_2 p_1 + K_{21}\overline{U}_2 & -K_{21}\overline{Y}_1 p_2 + K_{12}\overline{U}_1 & -p_3 \end{bmatrix} \begin{bmatrix} y_1 \\ y_2 \\ y_3 \end{bmatrix}$$
$$\equiv F_{(3 \times 3)}y_{(3 \times 1)}$$
$$(6)$$

Replacing $[u'_1, u'_2, u'_3]^T$ of Eq. (4) by Eq. (6), one has

$$\dot{X}_{(n \times 1)} = [A_{(nxn)} + B_{(n \times 3)}F_{(3 \times 3)}(I - D_{(3 \times 3)}F_{(3 \times 3)})^{-1}]X_{(n \times 1)} = \tilde{A}_{(n \times n)}X_{(n \times 1)}$$
$$y_{(3 \times 1)} = (I - D_{(3x3)}F_{(3 \times 3)})^{-1}C_{(3 \times n)}X_{(n \times 1)}$$
$$(7)$$

The term $B_{(n \times 3)}F_{(3 \times 3)}(I - D_{(3 \times 3)}F_{(3 \times 3)})^{-1}$ in Eq. (7) is the decoupling matrix. It includes designing parameters $K_{ij,i \neq j}$. For strict proper system, decoupling matrix becomes $B_{(n \times 3)}F_{(3 \times 3)}$. If state

variables are decomposed into three sets; i.e., $X_{(nx1)} = [X_1 | X_2 | X_3]^T$, and those are relate to three channels respectively, then Matrix $\tilde{A}_{n \times n}$ can be decomposed into nine sub-matrices; i.e.,

$$\tilde{A}_{(n \times n)} = \begin{bmatrix} \tilde{A}_{11} & \tilde{A}_{12} & \tilde{A}_{13} \\ \tilde{A}_{21} & \tilde{A}_{22} & \tilde{A}_{23} \\ \tilde{A}_{31} & \tilde{A}_{32} & \tilde{A}_{33} \end{bmatrix} \qquad (8)$$

where $\tilde{A}_{ij,i \neq j}$ are coupling matrices between channels. Exact decoupling can be obtained by nulling elements of coupling matrices. Eq. (3) gives there are only six parameters can be used. Thus, exact decoupling is impossible for system order $n > 3$. The number of parameters $K_{ij,i \neq j}$ is $m^2 - m$ for $m \times m$ multivariable systems and maximal total number of $\tilde{A}_{ij,i \neq j}$ is $n^2 - n$. In general, the value of $n^2 - n$ is greater than that of $m^2 - m$. It will be seen that eliminating/ reducing the major coupling elements in $\tilde{A}_{ij,i \neq j}$ to get diagonal dominant is rather than exact decoupling. Diagonal dominant can be obtained by minimizing off-diagonal norm/ diagonal norm ratios:

$$\min_{K_{ij,i \neq j}} \left\{ \sum_{i=1}^{3} \left[\sum_{j=1}^{3} \frac{\|\tilde{A}_{ij}\|}{\|\tilde{A}_{ii}\|} \right] \right\} \qquad (9)$$

Minimal-order model of the system will be used in the following section to find $K_{ij,i \neq j}$ first, and then hardware dynamic and compensations included for confirming effectives of decoupling characteristics of the complete system. Since PI controller can be used to decouple in low frequency band, thus the major effort will be paid to consider characteristics in medium frequency band. The detailed analyzed procedures and effectives will be illustrated by a 3×3 supersonic-missile flight control system. The minimal system order n to describe the flight control system is equal to 5.

III. Application to Flight Control Systems

The translational and rotational dynamics of the missile shown in Fig.1 are described by the following six nonlinear differential equations [19]:

$$\dot{U} = -\overline{q}\overline{s}C_x/m - WQ + VR + F_{xg}/m \qquad (10)$$

$$\dot{V} = -\overline{q}sC_y/m - UR + WP + F_{yg}/m \tag{11}$$

$$\dot{W} = -\overline{q}sC_z/m - VP + UQ + F_{zg}/m \tag{12}$$

$$\dot{P} = -C_l\overline{q}sl/I_x \tag{13}$$

$$\dot{Q} = C_m\overline{q}sl - (I_x - I_z)PR/I_y \tag{14}$$

$$\dot{R} = C_n\overline{q}sl - (I_y - I_x)PQ/I_y \tag{15}$$

In above equations, U, V and W are velocity components measured on the missile body axes; P, Q and R are the components of the body angular rate: F_{xg}, F_{yg}, F_{zg} are the gravitational forces acting along the body axes: and I_x, I_y, I_z are the moments of inertia. The variable $\overline{s}$ is the reference area, $\overline{q}$ is the dynamic pressure:

$$\overline{q} = \rho(U^2 + V^2 + W^2)/2 \equiv \rho V_M^2/2 \tag{16}$$

l is the reference length. The aerodynamic lifting forces (C_x, C_y, C_z) and moments (C_l, C_m, C_n) are function of Mach number, angle of attack (α^*), angle of sideslip (β^*); the angles of attack and sideslip are defined as

$$\alpha^* = \tan^{-1}(W/U) \tag{17}$$
and

$$\beta^* = \tan^{-1}[\sin^{-1}(V/V_M)/\cos\alpha^*] \tag{18}$$

The small signal perturbation model from a specified set of trim conditions ($P^*, Q^*, R^*, A_{ZO}, A_{YO}, \alpha^*, \beta^*$) is described by following differential equations:

$$\dot{p} = L_p p + L_\alpha \alpha + L_\beta \beta + L_{\delta p}\delta p + L_{\delta q}\delta q + L_{\delta r}\delta r \tag{19}$$

$$\dot{q} = M_q q + M_\alpha \alpha + M_{\delta q}\delta q + M_{\delta p}\delta p \tag{20}$$

$$\dot{\alpha} = -\tan\beta^* p + q + M_B(Z_\alpha \alpha + Z_{\delta q}\delta q + Z_{\delta p}\delta p) \tag{21}$$

$$\dot{r} = N_r r + N_\beta \beta + N_{\delta r}\delta r + N_{\delta p}\delta p \tag{22}$$

$$\dot{\beta} = \tan\alpha^* p - r + M_B(Y_\beta \beta + Y_{\delta r}\delta r + Y_{\delta p}\delta p) \tag{23}$$

$$a_{zacc} = Z_\alpha \alpha + Z_{\delta q}\delta q + Z_{\delta p}\delta p - l_S(M_q q + M_\alpha \alpha + M_{\delta p}\delta p + M_{\delta q}\delta q) \tag{24}$$

$$a_{yacc} = Y_\beta \beta + Y_{\delta r}\delta r + Y_{\delta p}\delta p + l_S(N_r r + N_\beta \beta + N_{\delta p}\delta p + N_{\delta r}\delta r) \tag{25}$$

where p, q, r are body angular rate deviations from trims (P^*, Q^*, R^*); a_{zacc}, a_{yacc} are body acceleration deviations from trims (A_{ZO}, A_{YO}); and α and β are angles of attack and sideslip deviations from trims (α^*, β^*), l_S is the distance between sensor position and Central of Gravity (CG). $L_{(\bullet)}, M_{(\bullet)}, N_{(\bullet)}$, $Y_{(\bullet)}$ and $Z_{(\bullet)}$ are derivatives of moments (C_l, C_m, C_n)/ forces (C_y, C_z) with respect to p, q, r, α, β , $\delta p, \delta q, \delta r$. Fig. 2 shows connections given by Eqs. (19) to (25), in which gray blocks show coupling effects between rolling/ yawing/ pitching channels. For large angle of attack (α^*) and small sideslip angle (β^*), the magnitude of terms $\tan\beta^*$ and L_α will much less than those of $\tan\alpha^*$ and L_β, thus the original 3×3 system can be decomposed into a 2×2 roll-yaw coupled system and a pitching system. Similar to the case of large value of β^* and small value of α^* , it can be decomposed into a 2×2 roll-pitch coupled system and a yawing system.

Now, consider the major coupling effects from yawing channel to rolling channel of a 2×2 roll-yaw coupled system. The transfer function of $p/\delta r$ is

$$\frac{p}{\delta r} = \frac{L_{\delta r}s^2 + [L_\beta M_B Y_{\delta r} - L_{dr}(N_r + M_B Y_\beta)]s - L_\beta(N_{\delta r} + Y_{\delta r}M_B N_r)}{\begin{array}{c}s^3 - (L_p + N_r + M_B Y_\beta)s^2 + (L_p N_r + N_\beta + L_p M_B Y_\beta + N_r M_B Y_\beta - \tan\alpha^* L_\beta)s \\ + L_{\delta r}(N_\beta + N_r M_B Y_\beta) \\ \hline -L_p(N_\beta + N_r M_B Y_\beta) + N_r \tan\alpha^* L_\beta\end{array}} \tag{26}$$

The denominator of Eq. (26) can be approximated by

$$\Delta_{pr}(s) = s^3 - (L_p + N_r + M_B Y_\beta)s^2 + (N_\beta - a^* L_\beta)s - L_p N_\beta + N_r a^* L_\beta \tag{27}$$

for

$$\tan\alpha^* \cong a^*;$$
$$|N_\beta - \alpha^* L_\beta| >> |L_p N_r + L_p M_B Y_\beta|;$$
$$|-L_p N_\beta + N_r \alpha^* L_\beta| >> |L_p N_r M_B Y_\beta|$$

Since the value of N_r is negative for stable static margin(SM) of the missile, the positive value of $\alpha^* L_\beta$ is called the unstable aerodynamic coupling for it will destabilize or degrade performance of the system; while negative value of $\alpha^* L_\beta$ is called the stable aerodynamic coupling. Note that the magnitude of L_β given in the numerator of Eq. (26) is much greater than that of $L_{\delta r}$. Such that L_β and $\alpha^* L_\beta$ are two major coupling terms. They affect not only the magnitude but also the stability of the system.

6

Considering another simplified 2×2 roll-pitch coupled system, the transfer function of $p/\delta q$ is in the form of

$$\frac{p}{\delta q} = \frac{L_{\delta q} s^2 + [L_\alpha M_B Z_{\delta q} - L_{dq}(M_q + M_B Z_\alpha)]s + L_\alpha(M_{\delta q} - Z_{\delta q} M_B M_q)}{s^3 - (L_p + M_q + M_B Z_\alpha)s^2 + (L_p M_q - M_\alpha + L_p M_B Z_\alpha + M_q MBZ_\alpha - \tan\beta^* L_\alpha)s}$$

$$\frac{+L_{\delta q}(-M_\alpha + M_q M_B Z_\alpha)}{-L_p(-M_\alpha + M_q M_B Z_\alpha) - M_q \tan\beta^* L_\alpha}$$

(28)

Similar to discussions for the 2×2 roll-yaw coupled system, one can find the approximated denominator of Eq. (28) is

$$\Delta_{pq}(s) = s^3 - (L_p + M_q + M_B Z_\alpha)s^2 + (-M_\alpha + \beta^* L_\alpha)s + L_p M_\alpha - M_q \beta^* L_\alpha$$

(29)

Eq. (29) gives the positive value of $\beta^* L_\alpha$ is called the stable aerodynamic coupling; and negative value of $\beta^* L_\alpha$ is called the unstable aerodynamic coupling. $\beta^* L_\alpha$ and L_α are two major coupling terms from pitching channel to rolling channel. Eqs. (26) and (28) give that the characteristic of the considered system is largely affected by $\beta^* L_\alpha$ and $\alpha^* L_\beta$. These imply that uses of $U_2 Y_3$ and $U_3 Y_2$ in Eq. (3) are rather than those of $U_2 Y_2$, and $U_3 Y_3$ for decoupling flight control systems.

There are five measurable datum ($A_{YF}, A_{ZF}, P_f, Q_f, R_f$) and three controllable output commands ($\Delta_p, \Delta_q, \Delta_r$) of autopilot can be used for decoupling. Fig.3 excluding decoupling blocks is the well-proven control configuration of conventional missile autopilot [3, 4]. Consider the nonlinear decoupling configuration shown in Fig.3. The mathematical representation of the decoupling block is

$$\Delta'_p = \Delta_p + K_{32} A_{ZF} \times \Delta_r + K_{23} A_{YF} \times \Delta_q$$

(30)

$$\Delta'_q = \Delta_q + K_{13} A_{YF} \times \Delta_p$$

(31)

$$\Delta'_r = \Delta_r + K_{12} A_{ZF} \times \Delta_p$$

(32)

where $\Delta_{(\bullet)}$ terms are output commands of autopilot without decoupling, $\Delta'_{(\bullet)}$ terms are output commands with decoupling, and K_{32}, K_{23}, K_{13} and K_{12} are gains of decoupling loop to be found and applied. Since the maneuvers of pitching and yawing channels are orthogonal. There is almost no coupling between

pitching and yawing channels. Thus, Eqs. (31) and (32) neglect $A_{ZF} \times \Delta_r$ and $A_{YF} \times \Delta_q$.

The small signal perturbed equations of Eqs. (30) to (32) on trim conditions ($A_{ZO}, A_{YO}, \delta qo, \delta ro$) are

$$\delta p' = \delta p + K_{32}(A_{ZO}\delta r + a_{zacc}\delta ro) + K_{23}(A_{YO}\delta q + a_{yacc}\delta qo)$$

(33)

$$\delta q' = \delta q + K_{13} A_{YO}\delta p$$

(34)

$$\delta r' = \delta r + K_{12} A_{ZO}\delta p$$

(35)

with

$\Delta_p = \delta po + \delta p; \Delta_q = \delta qo + \delta q; \Delta_r = \delta ro + \delta r; A_{YF} = A_{YO} + a_{yacc};$,

$A_{ZF} = A_{ZO} + a_{zacc}$ and $\delta po \equiv 0$ for skid to turn missile. Signal flows with Eqs.(33) to (35) are given in Fig.4. Note that ($\delta p, \delta q, \delta r$) will replace ($\delta pc, \delta qc, \delta rc$) in following analyses, those are outputs of de-mixer of four actuators cascaded to ($\delta_{1c}, \delta_{2c}, \delta_{3c}, \delta_{4c}$) shown in Fig.3. Fig.4 shows the linearized control configuration for analyses and designs. Eq. (33) includes $A_{ZO}\delta r$ and $A_{YO}\delta q$. It implies that proper values of K_{32} and K_{23} may decouple the coupling terms $\alpha^* L_\beta$ and $\beta^* L_\alpha$. The uses of Eqs. (34) and (35) with proper values of K_{13} and K_{12} are used to decouple the kinematical coupling. For simplicity, hardware dynamics and compensations are first neglected to derive close-form solutions of K_{32}, K_{23}, K_{13} and K_{12}.

Since gain crossover frequencies of inner loops in conventional designs are usually greater than those of outer loops, outer loops shown in Fig.4 can be neglected for decoupling analyses and designs. This simplification will be verified by frequency and time responses of the complete system. The inputs of the plant of inner loops closed system can be written as below:

$$\delta p' = -K_{ip}p + K_{32}(A_{ZO}\delta r + a_{zacc}\delta ro) + K_{23}(A_{YO}\delta q + a_{yacc}\delta qo)$$

(36)

$$\delta q' = K_{iq}q + K_{13} A_{YO}\delta p$$

(37)

$$\delta r' = K_{ir}r + K_{12} A_{ZO}\delta p$$

(38)

Substituting terms (a_{zacc}, a_{yacc}) of Eq. (36) with Eqs. (24) and (25), one has

$$\begin{bmatrix} \delta p' \\ \delta q' \\ \delta r' \end{bmatrix} = \begin{bmatrix} e_{11} & e_{12} & e_{13} & e_{14} & e_{15} \\ 0 & e_{22} & 0 & 0 & 0 \\ 0 & 0 & 0 & e_{24} & 0 \end{bmatrix} \begin{bmatrix} p \\ q \\ \alpha \\ r \\ \beta \end{bmatrix} + \begin{bmatrix} f_{11} & f_{12} & f_{13} \\ f_{21} & 0 & 0 \\ f_{31} & 0 & 0 \end{bmatrix} \begin{bmatrix} \delta p \\ \delta q \\ \delta r \end{bmatrix}$$

(39)

where $e_{11} = -K_{ip}$;

$e_{12} = -K_{32}\delta rol_S M_q$; $e_{13} = +K_{32}\delta ro(Z_\alpha - l_S M_\alpha)$;

$e_{14} = +K_{23}\delta qol_S N_r$

$e_{15} = +K_{23}\delta qo(Y_\beta + l_S N_\beta)$; $e_{22} = K_{iq}$; $e_{34} = K_{ir}$

$f_{11} = K_{32}\delta roZ_{\delta p} + K_{23}\delta qoY_{\delta p}$; $f_{12} = K_{32}\delta ro(Z_{\delta q} - l_S M_{\delta q}) + K_{23}A_{YO}$;

$f_{13} = K_{32}A_{ZO} + K_{23}\delta qo(Y_{\delta r} + l_S N_{\delta r})$; $f_{21} = K_{13}A_{YO}$; $f_{31} = K_{12}A_{ZO}$

The simplified system will be closed after $(\delta p', \delta q', \delta r')$ are replace by $(\delta p, \delta q, \delta r)$. It implies

$$\begin{bmatrix} \delta p \\ \delta q \\ \delta r \end{bmatrix} = \frac{1}{\Delta_F} \begin{bmatrix} 1 & f_{12} & f_{13} \\ f_{21} & 1-f_{11}-f_{13}f_{31} & f_{13}f_{21} \\ f_{31} & f_{12}f_{31} & 1-f_{11}-f_{12}f_{21} \end{bmatrix} \begin{bmatrix} e_{11} & e_{12} & e_{13} & e_{14} & e_{15} \\ 0 & e_{22} & 0 & 0 & 0 \\ 0 & 0 & 0 & e_{34} & 0 \end{bmatrix} \begin{bmatrix} p \\ q \\ \alpha \\ r \\ \beta \end{bmatrix}$$

(40)

where

$$\Delta_F = 1 - k_{32}\delta_{\gamma o}Z - K_{23}\delta_{qo}Y_{\delta p} - K_{13}A_{YO}[K_{32}(Z_{\delta q} - l_S M_{\delta q}) + K_{23}A_{ZO}] - K_{12}A_{ZO}[K_{32}A_{ZO} + K_{23}(Y_{\delta r} + l_S N_{\delta r})]$$

(41)

Substituting Eq. (40) into Eqs. (19) to (23), one has

$$\begin{bmatrix} \dot{p} \\ \dot{q} \\ \dot{\alpha} \\ \dot{r} \\ \dot{\beta} \end{bmatrix} = \begin{bmatrix} a_{11} & a_{12} & a_{13} & a_{14} & a_{15} \\ a_{21} & a_{22} & a_{23} & a_{24} & a_{25} \\ a_{31} & a_{32} & a_{33} & a_{34} & a_{35} \\ a_{41} & a_{42} & a_{43} & a_{44} & a_{45} \\ a_{51} & a_{52} & a_{53} & a_{54} & a_{55} \end{bmatrix} \begin{bmatrix} p \\ q \\ \alpha \\ r \\ \beta \end{bmatrix}$$

(42)

Eq. (42) is the state transition matrix of the closed-loop system. Considering following five elements of above state-transition matrix for decoupling:

$a_{11} = L_p - K_{ip}[L_{\delta p} + K_{13}L_{\delta q}A_{YO} + K_{12}L_{\delta r}A_{ZO}]/\Delta_F$ (43)

$a_{13} = L_\alpha + K_{32}\delta ro(Z_\alpha - l_S M_\alpha)[L_{\delta p} + K_{13}L_{\delta q}A_{YO} + K_{12}L_{\delta r}A_{ZO}]/\Delta_F$ (44)

$a_{15} = L_\beta + K_{23}\delta qo(Y_\beta + l_S N_\beta)[L_{\delta p} + K_{13}L_{\delta q}A_{YO} + K_{12}L_{\delta r}A_{ZO}]/\Delta_F$ (45)

$a_{21} = K_{ip}[-M_{\delta p} + K_{13}M_{\delta q}A_{YO}]/\Delta_F$ (46)

$a_{31} = K_{ip}[-N_{\delta p} + K_{12}N_{\delta r}A_{ZO}]/\Delta_F$ (47)

where a_{13} is the state transition from α to $\dot{p}$ and a_{15} is the state transition from β to $\dot{p}$. Conventional design

concepts are to minimize ratios of $|a_{13}/a_{11}|$ and $|a_{15}/a_{11}|$ for diagonal dominant. It implies that larger value of K_{ip} and large gain crossover frequency of inner loop will be. Eqs. (44) and (45) represent that one can set a_{13} and a_{15} to be zeros (or approaching to zeros) with proper values of K_{32}, K_{23}, K_{13} and K_{12} . It minimizes ratios of $|a_{13}/a_{11}|$ and $|a_{15}/a_{11}|$ while leaving K_{ip} be alone. After a_{13} and a_{15} are set to be zeros, aerodynamic couplings (L_α and L_β) form pitching/ yawing channels to rolling channel can be eliminated. In another way, let a_{21} and a_{31} to be zeros, then kinematical coupling from p to $\dot{q}$ / or to $\dot{r}$ will be eliminated also. Then, the cycling of coupling between rolling and pitching/ yawing channels are disconnected. Note that the eliminations are not exact for the real system. However, small ratios of $|a_{13}/a_{11}|$ and $|a_{15}/a_{11}|$ are usually obtained for diagonal dominant. It is due to the Eq. (42) is derived on some simplifications and assumptions, and due to modeling uncertainties for aerodynamics are always exist.

The four decoupling loop gains K_{32}, K_{23}, K_{13} and K_{12} are found by setting four elements a_{13}, a_{15}, a_{21} and a_{31} to be zeros. They are in the form of

$$K_{32} = -\frac{L_\alpha\Delta_F}{\delta ro(Z_\alpha - l_S M_\alpha)[L_{\delta p} + K_{13}L_{\delta q}A_{YO} + K_{12}L_{\delta r}A_{ZO}]}$$

(48)

$$K_{23} = -\frac{L_\beta\Delta_F}{\delta qo(Y_\beta + l_S N_\beta)[L_{\delta p} + K_{13}L_{\delta q}A_{YO} + K_{12}L_{\delta r}A_{ZO}]}$$

(49)

$$K_{13} = \frac{M_{\delta p}}{M_{\delta q}A_{YO}}$$

(50)

$$K_{12} = \frac{N_{\delta p}}{N_{\delta r}A_{ZO}}$$

(51)

where Δ_F is given in Eq. (41). Eqs. (48) to (51) give K_{32}, K_{23}, K_{13} and K_{12} are independent on inner loop gains K_{ip}, K_{iq} and K_{ir} . They are functions of trim conditions ($A_{ZO}, A_{YO}, \delta qo, \delta ro$). By experience, the modeling uncertainties for aerodynamic coefficients are magnitudes of them rather than wrong signs of them. Wrong decoupling gains in sign can be avoided. This is the major advantage of the proposed method rather than dynamic inversions for matrix inversion of an incompletely known design model may introduce

6

wrong way cancellation. Another advantage is magnitudes of decoupling are adjusted automatically on those of (A_{ZF}, A_{YF}). It will be seen that gains found for large aerodynamic coupling condition can be used for small aerodynamic coupling conditions.

IV. A Supersonic Missile Example

The small perturbed aerodynamic coefficients of the considered system are given in Appendix A [20, 21] for seven combinations of angle of attacks (α^*) and sideslip (β^*). It gives that performance and robustness of the considered system will be affected by L_β for maximal value of coupling coefficient L_β is about two third of $L_{\delta p}$. In general, three SISO systems are designed first individually; i.e.,

$$\frac{p}{\delta p} = \frac{L_{\delta p}}{s - L_p} \tag{52}$$

for rolling channel;

$$\frac{q}{\delta q} = \frac{M_{\delta q}s - M_{\delta q}M_B Z_\alpha + Z_{\delta q}M_B Z_\alpha}{s^2 + (-M_q - M_B Z_\alpha)s + (-M_\alpha + M_q M_B Z_\alpha)} \tag{53}$$

$$\frac{a_{zcg}}{\delta q} = \frac{Z_{\delta q}s^2 - Z_{\delta q}M_q s + (M_{\delta q}Z_\alpha - Z_{\delta q}M_\alpha)}{s^2 + (-M_q - M_B Z_\alpha)s + (-M_\alpha + M_q M_B Z_\alpha)} \tag{54}$$

for pitching channel;

$$\frac{r}{\delta r} = \frac{N_{\delta r}s - N_{\delta r}M_B Y_\beta + N_{\delta r}M_B N_\beta}{s^2 + (-N_r - M_B Y_\beta)s + (N_\beta + N_r M_B Y_\beta)} \tag{55}$$

$$\frac{a_{ycg}}{\delta r} = \frac{Y_{\delta r}s^2 - Y_{\delta r}N_r)s + (-N_{\delta r}Y_\beta + Y_{\delta r}N_\beta)}{s^2 + (-N_r - M_B Y_\beta)s + (N_\beta + N_r M_B Y_\beta)} \tag{56}$$

for yawing channel and then connected them with aerodynamic / kinematical coupling terms ; i.e., MIMO system, for verification the suitability of SISO designs. Several iterations are usually needed. Table 1 gives SISO designed and MIMO analyzed results. The gains (K_{op}, K_{ip}, K_{oq}, W_{iq}, K_{iq}, K_{or}, W_{ir}, K_{ir}) are give in Appendix A. There are gain adjusting logics for rolling channel gains K_{ip} and K_{op}:

$Sckip = 0.025 |A_{ZO}| + 1.4; K_{ip} = Sckip \times K_{ipo}$;

$Sckop = 0.050 |A_{ZO}| + 1.4; K_{op} = Sckop \times K_{opo}$;

The use of *Sckip* and *Sckop* is to increase low frequency gain for coping with aerodynamic couplings. They are functions of A_{ZO}. The use of *Sckip* will increase the gain crossover frequency for large value of A_{ZO}. The use of *Sckop* will increase Low Frequency Gain Margins(LFGMs) while losing Phase Margin(PM) and keeping gain crossover frequency(WCR) almost be unchanged.

The compensators and hardware dynamics are given in Appendix B on s-domain. Digital compensators are derived from bilinear transformation: $s = 2(z-1)/T_s(z+1)$. From Table 1, one can see that it is a good design for good robustness found for SISO System; but LFGMs are reduced incrementally for larger coupling term added; i.e., MIMO system. The effects of coupling terms for (α^*, β^*) = (12°, 1°) are shown in Fig.5. Fig.5 shows open-loop frequency responses of the rolling channel. The broken point is at the position between δpc and actuator. The solid- lines are frequency responses of the rolling SISO system, and the doted-lines are those of 3×3 MIMO system while being broken the rolling inner loop only. Fig.5 shows that loop gain in low-medium frequencies is largely reduced by introducing coupling terms. Eqs. (26) and (28) give same conclusion. The corresponding LFGMs, High frequency Gain Margins (HFGMs) and PMs are all given in Table 1. It gives that LFGMs are unacceptable for $\alpha^* > 6°$. Furthermore, the system is nearly unstable for $\alpha^* \geqq 12$ °. Table 1 gives decoupling for better LFGMs is expected.

Table 2 gives the analyzed results with decoupling added. K_{32}, K_{23}, K_{13} and K_{12} are found by Eqs. (48) to (51). It gives LFGMs become acceptable (LFGM $\leqq$ 0.53), while keeping PMs and HFGMs almost be unchanged. The effective of decoupling is shown in Fig.5 (dashed-line) also. It recovers the magnitude from coupled system (doted-line) to increase LFGMs. Note that the effective for decoupling of two-axis maneuvering (α^*, β^*)=(10°, 8°) are given in Tables 1 and 2 also. Note also that K_{32}, K_{23}, K_{13} and K_{12} are found from simplified system without compensations and hardware dynamics. The effects of compensations and hardware dynamics must be analyzed.

Fig.6 shows the variation analyses for four combination conditions with/ without decoupling and with/without compensations and hardware dynamics. The doted-line shows the responses without decoupling/ without compensations and hardware dynamics. The dash-doted-line shows responses with decoupling/without compensations and hardware dynamics. The solid-line shows responses without decoupling/ with compensations and hardware dynamics. The dashed-line shows responses with decoupling/with compensations and hardware dynamics. Fig.6 shows that the decoupling characteristics are almost not affected by adding hardware dynamics and compensations. Hardware dynamics and compensations can be viewed as un-modeled dynamics. It implies that the proposed decoupling is robust for coping with un-modeled dynamics.

Table 3 gives the analyzed results with constant decoupling gains found for $(\alpha^*, \beta^*) = (12°, 1°)$. Other six trim conditions use same gains. It gives compatible results given in Table 2. For instance, HFGM and PM of the trim condition $(\alpha^*, \beta^*) = (1°, 1°)$ corresponding to $(A_{ZF}, A_{YF}) = (-1.42G, -1.42G)$ keep almost unchanged. Eq. (30) gives same conclusion for amplitudes of decoupling are adjusted by (A_{ZF}, A_{YF}) automatically. The decoupling described by $|K_{32}A_{ZO}\delta ro + K_{23}A_{YO}\delta qo|$ for each trim condition is given in Table 3. Over decoupling is avoided. The gain crossover frequency (WCR) of the rolling channel of each trim condition is given in Table 3 also. They are almost constant. The analyzed results gives in Table 3 show that decoupling are robust under large plant variations; i.e.; angle of attack (α^*) varied from 12° to. 1°. Appendix A gives variations of aerodynamic coefficients for seven trim conditions. Thus, constant gains K_{32}, K_{23}, K_{13} and K_{12} derived from serious aerodynamic coupling conditions can be used for all other trim conditions. All analyzed results are verified by 5-DOF simulations in following paragraphs.

Fig.7 shows the 5-DOF simulating results for $(A_{ZC}, A_{YC}) = (-22.3G, -1.42G)$ in absence of decoupling loops. The control configuration shown by Fig.3 excluding the proposed decoupling block is used in 5-DOF simulation. Output limitations for $(\delta pc, \delta qc, \delta rc)$ are $(\pm 5°, \pm 20°, \pm 20°)$. This operating condition is corresponding to trim condition $(\alpha^*, \beta^*) = (12°, 1°)$. Fig.7 shows the compensated system is nearly unstable for sustaining oscillating of A_{ZF}, P_F, R_F and β. The

oscillating frequency is 2.75Hz. Fig.6 gives same conclusion in frequency domain.

Fig.8 shows simulating results with decoupling described by Eqs. (30) to (32). It can be seen that the performance and stability of the system are improved significantly. The maximal value of rolling angular rate is equal to -15.6 deg/s. Note that constant decoupling gains given in Table 2 for $(\alpha^*, \beta^*) = (12°, 1°)$ are used in whole simulation. $\pm 5G$ varying testing for command A_{ZC} are applied after 2 seconds. It is corresponding to angle of attack (α^*) varying from 10° to 14°. These testing give decoupled behavior keeps almost unchanged for plant variations (emulating system uncertainties). Fig.9 shows simulation results for $(\alpha^*, \beta^*) = (1°, 1°)$ with decoupling gains found for $(\alpha^*, \beta^*) = (12°, 1°)$. It can be seen that over decoupling is avoided for small values of (A_{ZF}, A_{YF}) are used in decoupling loops.

V. Conclusions

In this literature, a nonlinear decoupling technique has been proposed to analyses and designs of multivariable feedback control systems. It was applied to a real 3×3 supersonic missile flight control system. No dynamic inversion is needed in analyses and designs. The close-form solutions of decoupling gains were found easily by a simplified system and verified by the complete system including hardware dynamics and compensations. The decoupling effects were kept almost unchanged for large system parameter variations and uncertainties. From 5-DOF simulation results, one can see that the proposed method gave a possible way to cope with aerodynamic coupling for high performance missile.

References

1. D. V. Stallard, Decoupling the Flight Control System of a Cruciform Missile, AIAA- Paper-76-1943, (1976) 236-246.

2. A. Arrow and D. J. Yost, Large Angle of Attack Missile Control Concepts for Aerodynamic Controlled Missiles, J. of Spacecraft, Vol.14, No.10, (1977) 606-613.

3. F. W. Nesline and P. Zarchan, Robust Instrumentation Configurations for Homing Missile Flight Control," AIAA Guidance Control Conference, AIAA-Paper-80-1749, (1980) 209-219.

4. F. W. Nesline and M. L. Nesline, How Autopilot Requirements Constraint the Aerodynamic Design of

Homing Missile, American Control Conference, (1984) 716-730.

5. E. Santis and A. Vicino, Diagonal Dominance for Robust Stability of MIMO Interval Systems, IEEE Transactions on Automatic Control, Vol.41, No.6, (1996) 871-875.

6. S. S. Chughtai and N. Munro, Diagonal Dominance Using LMIs, IEE Proceedings- Control Theory and Applications, Vol.151, no. 2, (2004) 225- 233.

7. B. D. O. Anderson and M. R. Gevers, On Multivariable Pole-zero Cancellations and Stability of Feedback Systems, IEEE Trans. on Circuit and System, Vol.28, No.8, (1981) 830-833.

8. A. Linnemann and R. Maier, Decoupling by Pre-compensation while Maintaining Stability, IEEE Trans. on Automatic Control, Vol.38, No.4, (1993) 629-632.

9. Q. G. Wang, and Y. Yang, Transfer Function Matrix Approach to Decoupling Problem with Stability, Systems and Control Letters, Vol.47, (2002) 103-110.

10. 10.S. N. Singh and W. J. Rugh, Decoupling in a Class of Nonlinear Systems by State Variable Feedback, Journal of Dynamic System, Measurement and Control, Vol.94, No.4, (1972) 323-329.

11. 11.C.A. Desoer and A. N. Gunds, Decoupling Linear Multiinput Multioutput Plant by Dynamic Output Feedback: an algebraic theory, IEEE Trans. on Automatic Control, Vol.31, (1986) 744-750.

12. 12. C. Snell, S. A., Englewood, D. F. Enns and W. L. Garrard, Nonlinear Inversion Flight Control for a Supermaneuver Aircraft, Journal of Guidance, Control and Dynamics Vol.15, No.4, (1992) 976-984.

13. 13.S. H. Lane and R. F. Stengel, Flight Control Design Using Nonlinear Inverse Dynamics, Automatica, Vol. 24, (1988) 471-484.

14. 14.D. D. Enns, R. Bugajski and G. Stein, Dynamic Inversion: an Evolving Methodology for Flight Control Design, Int. J. of Control, Vol.59, (1994).71-91.

15. 15. S. A. Snell and. P. W Stout, Flight Control Law Using Nonlinear Dynamic Inversion Combined With Quantitative Feedback Theory, Journal of Dynamic Systems, Measurement and Control, Vol.120, No.2, (1998) 208-214.

16. 16. W. Siwakosit, S. A. Snell and, R.A. Hess, Robust Flight Control Design with Handling Qualities Constraints using Scheduled Linear Dynamic Inversion and Loop-Shaping, IEEE Trans. on Control Systems Technology, Vol.8, No.3, (2000) 483-494.

17. J. Reiner, G. J. Balas and W. J. Garrard, Flight Control Design Using Robust Dynamic Inversion and Time-scale Separation, Automatica, Vol.32, No.11, (1996) 1493-1504.

18. R. J. Adams and S. S. Banda, Robust Flight Control Design Using Dynamic Inversion and Structured Singular Value Synthesis, IEEE Trans. on Control System Technology, Vo1.2, No.2, (1993) 80-92.

19. J. H. Blakelack, Automatic Control of Aircraft and Missile, Second Edition, John Wiley and Sons, New York, 1991.

20. W. J. Monta, Supersonic Aerodynamic Characteristics of An Air-to-air Missile Configuration with Cruciform Wings and In-line Tail Control, NASA- TM- X- 2666, Langley Research Center, Hampton, Virginia, 1972.

21. W. J. Monta, Supersonic Aerodynamic Characteristic of A Sparrow III Type Missile Model With Wing Control and Comparison with Existing Tail-control Results, NASA- TR- 1078, Langley Research Center, Hampton, Virginia, 1977.

Appendix A: Aerodynamic Coefficients and Loop Gains

Seven sets of aerodynamic coefficients and trim values (A_{zo}, A_{yo}, $\delta qo, \delta ro$) of an air-to-air missile [20, 21] at VM=676.8m/s are given below:

$L_{\delta q}$ =730.45	$L_{\delta p}$ =14609.0	$L_{\delta r}$ =730.45	L_p = -4.798	M_q =-3.232
N_r =-3.232	N_β =219.22	$N_{\delta r}$ =-599.7	$N_{\delta p}$ =-29.99	$Z_{\delta q}$ =-30.61
Y_β =-95.85	$M_{\delta q}$ =-599.7	$M_{\delta p}$ =-29.99	$Y_{\delta r}$ =30.611	$Y_{\delta p}$ = 0.000
K_{opo} =15.58	K_{ipo} =0.0031	K_{oq} =0.0744	W_{iq} =15.98	K_{iq} =0.0409
l_S =0.035	M_B =0.0145	K_{or} =0.0744	W_{ir} =15.98	K_{ir} =0.0409

A1.	α^* =12.00°	β^* =1.00°	L_α =684.45	L_β =8951.6	Z_α =-176.65
	M_α =-591.6	δro =0.46°	δqo =-11.33°	A_{YO} =-1.42G	A_{ZO} =-22.3G
A2.	α^* =10.00°	β^* =1.00°	L_α =809.8	L_β =7324.1	Z_α =-171.4
	M_α =-571.3	δro =0.46°	δqo =-8.86°	A_{YO} =-1.42G	A_{ZO} =-17.53
A3.	α^* =8.00°	β^* =1.00°	L_α =623.76	L_β =5787.7	Z_α =-161.45
	M_α =-508.7	δ_r^* =0.46°	δqo =-6.17°	A_{YO} =-1.42G	A_{ZO} =-13.1G
A4.	α^* =6.00°	β^* =1.00°	L_α =518.8	L_β =4446.8	Z_α =-136.9
	M_α =-392.8	δro =0.46°	δqo =-3.83°	A_{YO} =-1.42G	A_{ZO} =-9.11G
A5.	α^* =4.00°	β^* =1.00°	L_α =606.29	L_β =2835.8	Z_α =-109.16
	M_α =-252.4	δro =0.46°	δqo =-2.12°	A_{YO} = -1.42G	A_{ZO} =-5.77G
A6.	α^* =2.00°	β^* =1.00°	L_α =1510.1	L_β =-528.8	Z_α =-97.29
	M_α =-228.8	δro =0.46°	δqo =-2.13°	A_{YO} =-1.42G	A_{ZO} =-2.88G
A7.	α^* =1.00°	β^* =1.00°	L_α =2789.6	L_β = -2790	Z_α =-95.85
	M_α =-219.2	δro =0.46°	δqo =-0.46°	A_{YO} = -1.42G	A_{ZO} =-1.42G

Appendix B: Compensators and Hardware Dynamic Models

1. Rolling outer/inner loop compensators

$$POC(s) = K_{op}\frac{s/8.79+1}{s/4.4+1}, \quad PIC(s) = K_{ip}\frac{s/282.6+1}{s/1413+1}$$

2. Yawing/Pitching outer/inner loop compensators

$$ROC(s) = K_{or}\frac{s/18.84+1}{s/12.56+1}\cdot RSC(s) = \frac{W_{ir}}{s},$$

$$RIC(s) = K_{ir}\frac{s/157+1}{s/942+1}$$

$$QOC(s) = K_{oq}\frac{s/18.84+1}{s/12.56+1}\cdot QSC(s) = \frac{W_{iq}}{s},$$

$$QIC(s) = K_{iq}\frac{s/157+1}{s/942+1}$$

3. Actuator models

$$CAS(s) = \frac{166627}{s^2+142.9.5s+166627}$$

4. Rate gyro/accelerometer models

$$RG(s) = \frac{193444}{s^2+263.9s+193444}$$

5. Inner loop low-pass filter body angular rate

$$LPFI(s) = \frac{439.6}{s+439.6}$$

6. Outer loop low-pass filter for acceleration

$$LPFO(s) = \frac{251.2}{s + 251.2}$$

Table 1 SISO System and MIMO System without Decoupling

Trims	SISO System		MIMO without Decoupling		
α^* / β^*	HFGM	PM	LFGM	HFGM	PM
12°/1°	**1.84**	**55.4°**	**0.99**	**1.89**	**0.9°**
10°/1°	**1.96**	**57.5°**	**0.79**	**1.99**	**59.2°**
8°/1°	**2.09**	**59.4°**	**0.60**	**2.11**	**60.6°**
6°/1°	**2.22**	**61.2°**	**0.42**	**2.23**	**62.0°**
4°/1°	**2.34**	**62.7°**	**0.25**	**2.34**	**63.1°**
2°/1°	**2.46**	**64.0°**	**—**	**2.45**	**64.1°**
1°/1°	**2.52**	**64.7°**	**—**	**2.51**	**64.7°**
10°/8°	**1.96**	**57.5°**	**0.17**	**1.96**	**58.0°**

Table 2 MIMO System with Decoupling Loops and Found Gains.

Trims	Robustness			Decoupling Gains			
α^* / β^*	LFGM	HFGM	PM	K_{32}	K_{23}	K_{13}	K_{12}
12°/1	**0.54**	**1.95**	**38.4°**	**0.0366**	**-0.0341**	**0.0351**	**0.0022**
10°/1	**0.46**	**2.05**	**45.3°**	**0.0447**	**-0.0357**	**0.0351**	**0.0029**
8°/1°	**0.39**	**2.15**	**51.9°**	**0.0369**	**-0.0411**	**0.0351**	**0.0038**
6°/1°	**0.32**	**2.25**	**56.7°**	**0.0360**	**-0.0514**	**0.0351**	**0.0055**
4°/1°	**0.21**	**2.36**	**60.8°**	**0.0523**	**-0.0590**	**0.0351**	**0.0087**
2°/1°	**—**	**2.49**	**64.4°**	**0.1431**	**0.0245**	**0.0351**	**0.0176**
1°/1°	**—**	**2.57**	**65.7°**	**0.2630**	**0.2630**	**0.0351**	**0.0351**
10°/8	**0.13**	**1.98**	**57.5°**	**0.0303**	**-0.0176**	**0.0039**	**0.0029**

Table 3 MIMO System with Constant Decoupling Gains.

Trims	Robustness			Gain-Crossover	Decoupling
α^* / β^*	LFGM	HFGM	PM		$\lvert K_{32}A_{zo}\delta ro + K_{23}A_{yo}\delta qo \rvert$
12°/1°	**0.54**	**1.95**	**38.4°**	**10.5Hz**	$1.613 \times 10^{-2}\,G \cdot rad$
10°/1°	**0.47**	**2.05**	**46.2°**	**10.8Hz**	$1.264 \times 10^{-2}\,G \cdot rad$
8°/1°	**0.40**	**2.15**	**53.1°**	**11.0Hz**	$9.063 \times 10^{-3}\,G \cdot rad$
6°/1°	**0.33**	**2.26**	**58.2°**	**11.1Hz**	$5.913 \times 10^{-3}\,G \cdot rad$
4°/1°	**0.22**	**2.36**	**61.5°**	**11.2Hz**	$3.486 \times 10^{-3}\,G \cdot rad$
2°/1°	**—**	**2.46**	**63.6°**	**11.3Hz**	$1.633 \times 10^{-3}\,G \cdot rad$
1°/1°	**—**	**2.52**	**64.4°**	**11.1Hz**	$8.060 \times 10^{-4}\,G \cdot rad$

Fig.1 Coordinated System Definitions.

Fig.4 Linearized Control Configuration for Analyses and Designs.

Fig.2 Linear Perturbed Model of the missile.

Fig.5 Open-loop Bode Diagrams of Rolling Channel for (α^*, β^*)=(12°,1°).

Fig.3 Digital Autopilot with Nonlinear Feedback Decoupling Block.

Fig.6 Frequency Responses of p/Ayc for(α^*, β^*)=(12°,1°).

6
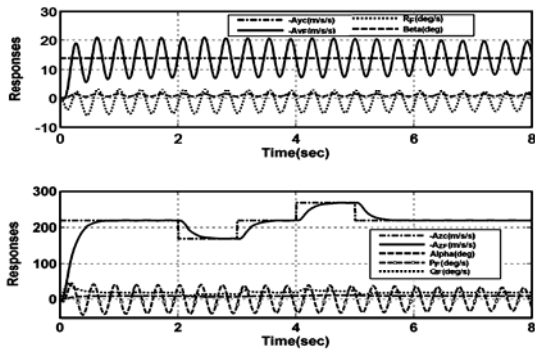
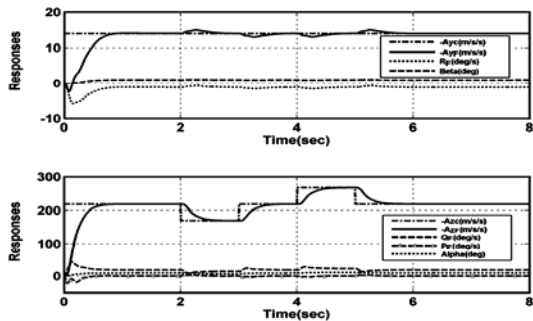**Fig.7 5-DOF Simulations of the system without Decoupling Loop.**

Fig.8 5-DOF Simulations of the system with Decoupling Loop.
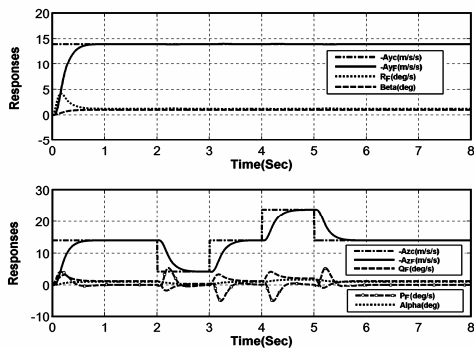

Fig.9 5-DOF Simulations of the system with Decoupling Loop.

多變數系統解耦與飛行控制系統應用

蔡添壽

國立虎尾科技大學飛機工程學系　助理教授

摘　　要

　　本文針對多變數系統提出一個非線性解耦連的分析與設計方法，此法被運用在一個氣動力耦連非常嚴重的超音速飛彈上。此法不需要系統動態特性的反矩陣進行解耦。從滾轉頻道的頻率響應及時間響應，可以得知解耦與穩健度可以同時達成，此法在大飛行包線之大參數變化下與模式不確定下仍能適用。

關鍵詞:多變數系統解耦連、飛行控制系統